Human Pathology (2019) **84**, 164–172

ELSEVIER

Human PATHOLOGY

www.elsevier.com/locate/humpath

Original contribution

Hydropic leiomyoma: a distinct variant of leiomyoma closely related to HMGA2 overexpression☆,☆☆,★

Brannan B. Griffin MD, Yanli Ban MD, Xinyan Lu MD, Jian-Jun Wei MD*

Department of Pathology, Northwestern University Feinberg School of Medicine, Chicago, IL 60611, USA

Received 19 August 2018; revised 22 September 2018; accepted 29 September 2018

Keywords:
Hydropic leiomyoma;
Histology;
HMGA2;
FISH;
Pericytes

Summary Hydropic leiomyoma (HLM) is a variant of uterine leiomyoma with characteristic features of zonal distributions of edema, increased vascularity, and tumor cells arranged in nodules or cords. Diagnostic difficulty and patient management are further complicated by a lack of studies and unknown cause of the disease. To study this tumor's nature, 24 HLM cases were selected for analysis of cytohistologic features, immunohistochemical profile (HMGA2, FH, CD34, pAKT, p16, ER, SMA, and Ki-67), and molecular alterations of *HMGA2* by fluorescence in situ hybridization and *MED12* mutations. HLM showed large tumor size (average 14.4 cm) and unique histology, characterized by edematous areas of tumor cells with mostly round-oval nuclei, arranged in cords and/or with perinodular growth around vessels, and increased thick-walled vessels (average 17 vessels/10× medium-power field). Immunohistochemistry revealed that 76% (18/24) of HLMs had HMGA2 overexpression, 32% (6/19) of which harbored *HMGA2* rearrangement detected by fluorescence in situ hybridization. Thick-walled vessels in HLM were composed of mostly HMGA2-positive tumor cells, and HLM with HMGA2 overexpression also showed CD34-positive tumor vessel–supporting pericytes. In contrast to usual-type leiomyoma with a high frequency of *MED12* mutations, no *MED12* mutations were found in any HLM. HLM showed increased pAKT activity, indicating a strong contribution of AKT pathway signaling in HLM promoting tumor growth. Our findings suggest that HLM is a distinct variant of uterine smooth muscle tumor likely driven by HMGA2 overexpression.

☆ Competing interests: The authors have disclosed that they have no significant relationships with, or financial interest in, any commercial companies pertaining to this article.

☆☆ Funding/Support: This study was supported in part by the National Institutes of Health (Grant P01HD57877) and the departmental trainee education fund of the Department of Pathology, Feinberg School of Medicine, and Northwestern University.

★ This study was presented at the 107th Annual Meeting of United States and Canadian Academy of Pathology on Monday March 19, 2018, in Vancouver, BC, Canada, and presented in part at Northwestern University Feinberg School of Medicine's 13th Annual Lewis Landsberg Research Day in April 2018.

* Corresponding author at: Department of Pathology, Northwestern Memorial Hospital, Northwestern University Feinberg School of Medicine, 251 East Huron St, Galter 7-334, Chicago, IL 60611.

E-mail address: jianjun-wei@northwestern.edu (J. -J. Wei).

https://doi.org/10.1016/j.humpath.2018.09.012

1. Introduction

Uterine leiomyoma is the most common benign neoplasm of the female reproductive system, and the incidence among the general population before menopause is up to 70%. Moreover, 20% to 40% of leiomyomata are symptomatic, often related to large tumor size, and most likely require surgical treatment [1]. Leiomyomata are histologically heterogeneous and multiple variants exist, with some showing features that obfuscate the smooth muscle nature of the neoplasm. Hydropic leiomyoma (HLM) is one of the aforementioned variants included in the most recent World Health Organization's classification (2014) of uterine mesenchymal tumors [2]. Although hydropic change has been a known feature of a subset of leiomyomas for many years, the article of Clement et al [3] and World Health Organization 2014 depicted a clear description of tumor-specific histology. This entity characteristically shows watery edema, increased vascularity, and tumor cells arranged in nodules or cords. All these features are seen in zonal distributions and thus can cause diagnostic difficulty, especially in cases with extensive hydropic change and concurrent loss of usual-type leiomyoma (ULM) architecture.

The majority of knowledge from the literature regarding HLM has come from case reports and series, with few being published in pathology-specific journals. This observation highlights the lack of awareness and clarity regarding the diagnosis of HLM. Pathological understanding of HLM is additionally complicated by an unknown etiology of tumorigenesis. Van den Berghe et al [4] found t(4;8)(p16;q22) as the sole chromosomal abnormality in the karyotype of a single HLM case. However, this result is neither reported elsewhere in the literature nor replicated in additional studies, to our knowledge. Given the little knowledge of HLM, and especially considering its significant clinical impact, we aim to increase awareness of HLM and clarify this unusual leiomyoma variant. Prior identification of several driver gene mutations in ULM provides a concept and tools for investigating HLM. In particular, ULMs with *HMGA2* alteration are shown to be relatively larger in size and have a more burdening clinical pattern [5,6]. We collected and analyzed 24 HLM cases for histology, immunohistochemistry (IHC), and molecular alterations in this study.

2. Materials and methods

2.1. Case selection

The study was approved by Northwestern University's institutional review board. We searched our institution's surgical pathology database of the prior 15 years (since 2003) for all variants of leiomyoma likely with increased vascularity, including angioleiomyoma, vascular leiomyoma, intravascular leiomyomatosis, HLM, and cotylednoid leiomyoma. Our search yielded 200 cases for review. Two pathologists then reviewed select representative hematoxylin and eosin–stained slides of tumor cases independently to ensure diagnostic agreement. Criteria for inclusion within our study were diffuse presence of HLM features previously established by Clement et al [3]. Twenty-four HLM cases met our inclusion criteria, and in addition, 21 ULM cases were included as controls for both morphologic comparison and ancillary testing. For each selected

Table Biomedical/paramedical and pathologic features and IHC of HLM and ULM

	HLM	ULM	*P*
Clinical and histology			
No. of cases	24	21	
Age (y), mean ± SD	43.79 ± 12.7	46.1 ± 6.2	.8912
Tumor size (cm), mean ± SD	14.4 ± 8.2	6.7 ± 0.8	.0425
Nuclear features	Small, round-oval	Spindle, cigar-shaped	
Nucleoli	Pinpoint	Conspicuous	
Thick-walled vessels (/10× mpf)	17 (range, 7-40)	9 (range, 0-21)	<.001
High edema/hydropic matrix	50% (12/24)	14% (3/21)	<.001
IHC			
HMGA2 positive (IHC)	18/24 (76%)	2/21 10%	<.001
HMGA2 translocation (FISH)	6/19 (32%)	0/5 (0%)	<.001
MED12 mutations	0/21 (0%)	15/21 (71%)	<.001
FH loss (IHC)	0/24 (0%)	0/21 (0%)	NS
pAKT intensity (IHC)	3.0 (2.25-2.95)	1.0 (1.20-1.66)	<.001
ER positivity % (IHC)	80 (62.8-85.2)	60 (50.4-60.9)	.004
CD34 (vessel density/mpf)	47 (range, 6-80)	22 (range, 5-106)	.0003
Ki-67 index (%)	4 (range, 1-20)	2 (range, 1.98-4.5)	.0210
Molecular analysis			
HMGA2 FISH	6/19 (32%)		
MED12 mutations	0/21 (0%)	15/21 (71%)	<.001

Abbreviation: NS, not significant.

case, we reviewed our institution's electronic medical record and pathology reports to obtain patient biodemographic and tumor specimen data.

2.2. Slide review and histologic parameters

We analyzed histologic features for each case recording extent of edema, vascular density, cellular growth pattern, and tumor cytology. Edematous change was evaluated across three medium-power fields (mpfs) and scored as follows: 0, absent/no edema; 1, minimal edema (<10%); 2, moderate edema (10%-50%); and 3, severe edema (>50%). Vascular density was evaluated across three 10× mpfs and counted as number of thick-walled vessels per mpf.

2.3. Immunohistochemistry

Using the collected tissue blocks, we prepared tissue microarrays (TMAs) of HLM, ULM, and myometrial controls using 2-μm representative tissue sections through Northwestern University's Path Core facilities. IHC was performed on the prepared TMAs for all 24 HLMs and 21 ULMs. The analytical markers used for IHC analysis included estrogen receptor (ER), fumarate hydratase (FH), high mobility group A (HMGA2), MED12, cell proliferative marker (Ki-67), AKT pathway marker (pAKT), CD34, and smooth muscle actin (SMA). All information on antibodies and stain conditions is summarized in Supplementary Table 1. All immunohistochemical staining procedures were performed on a Ventana Nexus automated system (Basel, Switzerland). Staining results were evaluated by 2 pathologists, and when applicable, the percent and intensity of relevant stains were assessed. Intensity was scored as negative (0), weak (1+), moderate (2+), or strong (3+), and percentage of positive tumor cells was scored from 0% to 100%. The results were then semiquantitatively analyzed. Vasculature density detected by CD34 was further evaluated in whole-mounted tumor sections in all cases.

2.4. Fluorescence in situ hybridization

Fluorescence in situ hybridization (FISH) break-apart probe for the *HMGA2* gene with the *5'HMGA2* labeled in spectrum-orange (5′ end) and *3'HMGA2* labeled in spectrum-green (Empire Genomics, Buffalo, NY) was used on TMA for both samples and controls to assess *HMGA2* gene rearrangement status and/or copy numbers. Probe integrity and localization were first evaluated on normal metaphase spreads from a peripheral blood sample by the Clinical Cytogenetics Laboratory at Northwestern Memorial Hospital. FISH signals were assessed at 100× hpf magnification to ensure intracellular location, and for each case or control, an attempt was made to count 200 cells in total. FISH patterns showing only yellow fusion signals with colocalized/direct juxtaposition of orange and green signals were scored as intact *HMGA2* and negative for gene rearrangement. Fusion signals coexisting with separate hybridization signals showing a single spectrum-green (1G) or spectrum-orange color (1R) were scored as positive for *HMGA2* gene rearrangement. Cells meeting this criterion often showed 1F/1R/1G, 1F/1G, or 1F/1R signals, and cases were scored as positive if a threshold of at least 10% was reached. Cases were excluded as uninterpretable if no signals could be visualized within the tumor tissue present.

2.5. *MED12* mutation analysis

Genomic DNA was extracted from tumor FFPE tissue sections with a DNA extraction kit (Qiagen, Boston, MA), and 50 ng of DNA was loaded into polymerase chain reaction. DNA from exon 2 of *MED12*, with flanking exon-intron junction sequences, was amplified with primers 5′-GCC CTT TCA CCT TGT TCC TT-3′ (forward) and 5′-TGT CCC TAT AAG TCT TCC CAA CC-3′ (reverse). Polymerase chain reaction products were purified by ExoSAP-IT reagent (Affymetrix, Santa Clara, CA) following the manufacturer's instructions.

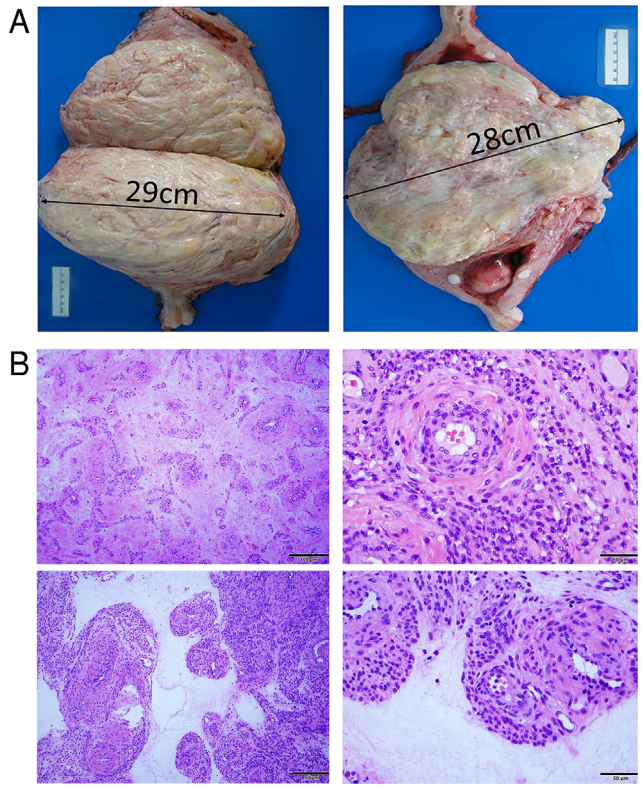

Fig. 1 Examples of photomacrographs (A) and photomicrographs (B) illustrate gross features of HLMs. A, Tumors are usually large intramural masses with a demarcated border. Cut surface reveals a relatively pale, white-pink, and light-yellow appearance with soft areas of watery edema and pinpoint hemorrhage. B, Photomicrographs illustrate the typical histologic features of HLM in low-power fields (left panels) and high-power fields (right panels). Tumor consists of a mixture of tumor cells around thick-walled vessels in the background of loose, hyalinized collagenous extracellular matrix. Magnification is indicated in the right lower corner by the black bar (50-100 μm).

Sequencing of the purified DNA products was performed at Northwestern University's NUSeq Core using Applied Biosystems' BigDye version 3.1 (ThermoFisher Scientific, Waltham, MA). The reactions were then run on Applied Biosystems' 3730xl DNA Analyzer. Mutations/variations were analyzed by DNASTAR Lasergene 9 software (Madison, WI).

2.6. Data interpretation and statistical analysis

GraphPad Prism version 6 (La Jolla, CA) software was used for statistical analysis. IHC data were presented as median and ranges for tumor samples and control myometrium; other data were presented as mean and SD. Either Student *t* test or 1-way analysis of variance was used to determine statistical significance, and a *P* value less than .05 was considered statistically significant.

3. Results

3.1. Clinical presentation

Women of similar, but overall younger, reproductive age were affected by HLM (average 43.79 ± 12.7 years) compared with ULM (average 46.1 ± 6.2 years; $P = .8912$; Table). Presentation data were available for 22 (92%) of 24 cases in our study. Most patients presented for menorrhagia, with some cases complicated by anemia requiring blood transfusion and iron deficiency requiring replacement, including infusion therapy. Other patient symptoms included abdominal and/or pelvic pain, feeling of pelvic fullness, abdominal distension, vaginal discharge, dysparenuria, urinary incontinence, constipation, fatigue, and decreased appetite with early satiety. One patient presented with the tumor as an incidental finding for workup of acute worsening of biliary-colic symptoms, and another one was an unexpected etiology of abdominal distension in early pregnancy. Two patients presented with possibly related infections as their primary medical problems, including hydronephrosis and urinary tract infection. Physical examination data conveyed nontender masses, with 4 patients having tumors prolapsing through cervical and/or vaginal oses. Imaging data showed large, heterogeneously contrast-enhancing masses that ranged from well delineated within the uterus to complex, exophytic, and indistinguishable from adnexae in 5 cases. Of note, 5 tumors showed overt cystic change; 2 described as degenerative, 1 associated with moderate free fluid in the pelvis, and 1 showing concurrent multiple pelvic lymphadenopathy (up to 3 cm in greatest dimension). Ten HLM cases occurred as single tumors, whereas 14 were seen in the setting of multiple ULM tumors.

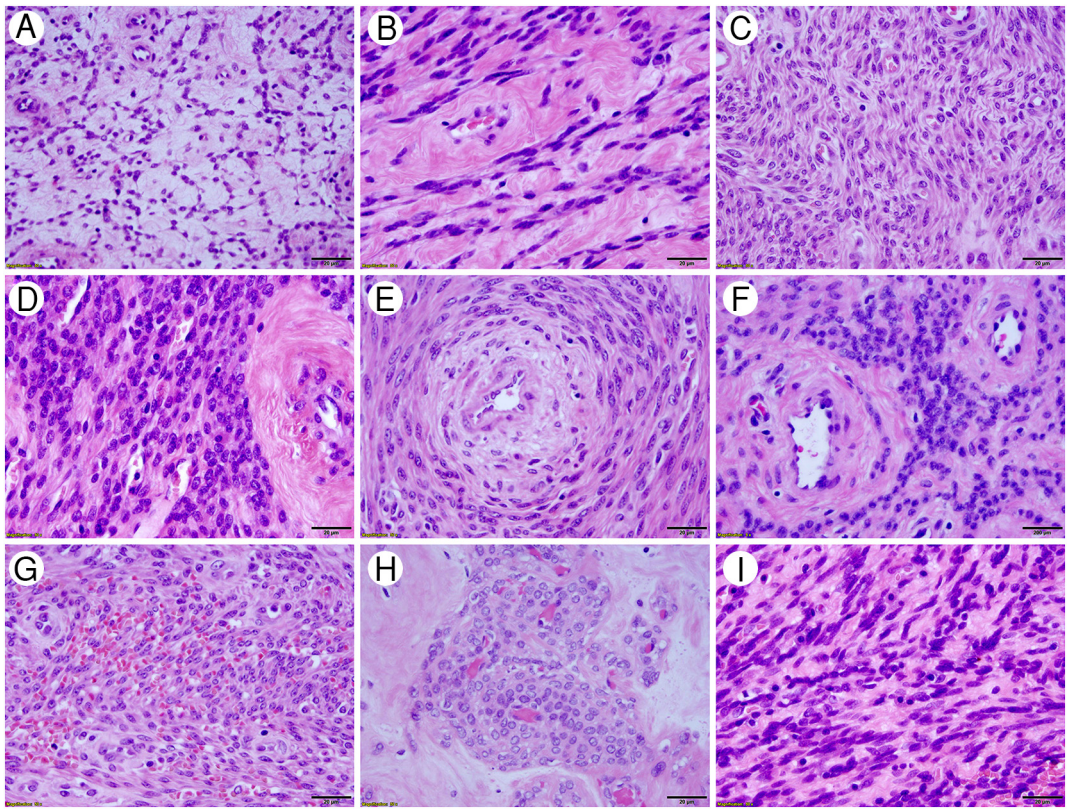

Fig. 2 Cytologic features of HLM. High-power fields in hematoxylin and eosin–stained slides reveal that HLMs have tumor cells predominantly with relatively small, round or oval nuclei. Tumor cells are seen in various tumor patterns as presented in reticulated (A), streaming (B), sheath-like (C), cellular (D), concentric (E), and perivascular (F) components, as well as with red blood cell extravasation (G), perivascular pseudonodules (H), and spindled (I) components. Magnification indicated in the right lower corner by the black bar (20 μm).

3.2. Pathologic features

HLM tumors showed larger size compared with ULM (average 14.4 ± 8.2 cm versus 6.7 ± 0.8 cm; $P = .0425$; Table). Gross features of HLM cases included well-demarcated, vaguely nodular to lobulated tumors with white-gray, watery edematous cut surfaces containing occasional pinpoint hemorrhage and granular texture (Fig. 1). No overtly necrotic tissue

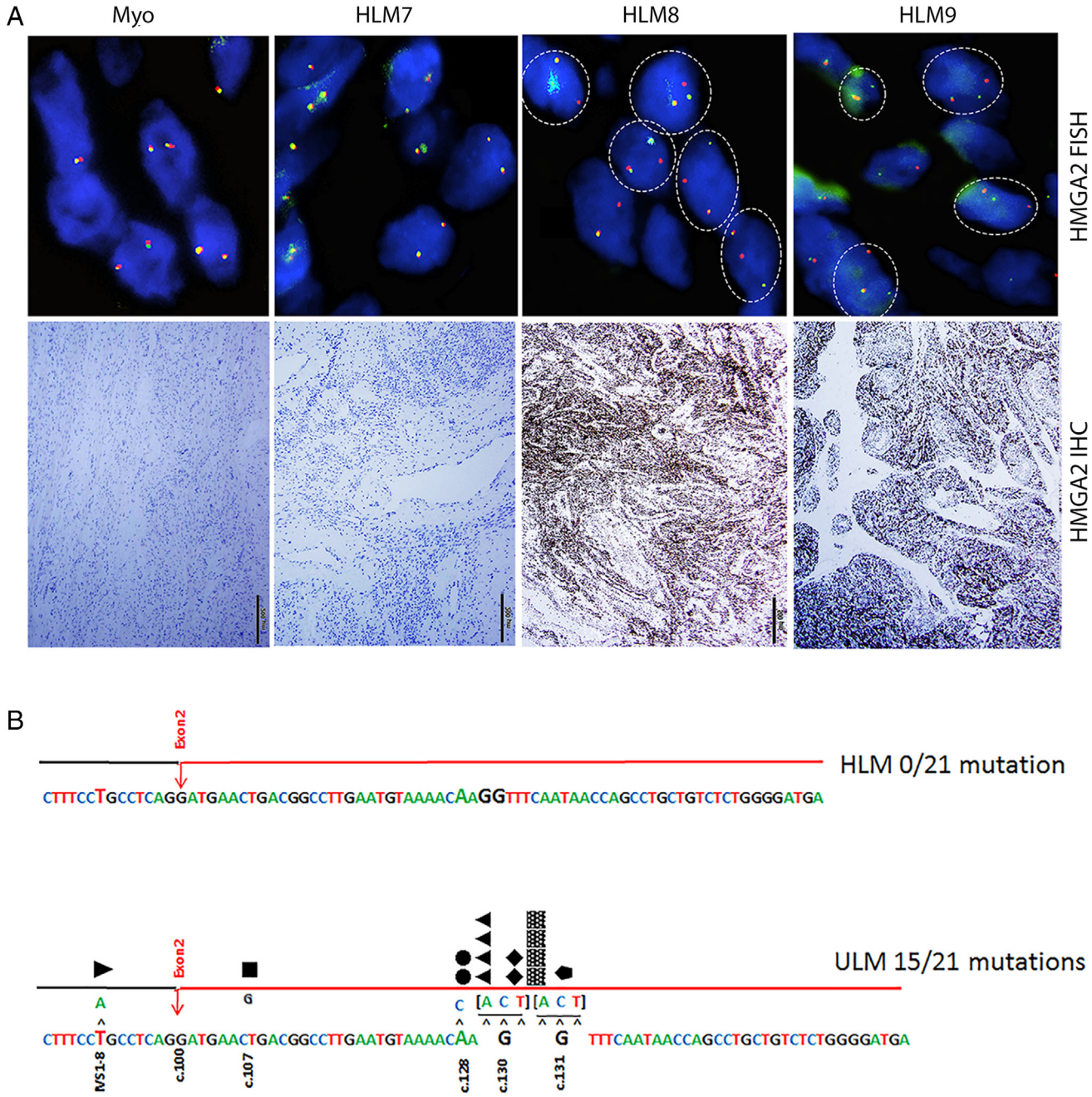

Fig. 3 Molecular analysis of *HMGA2* and *MED12* alterations in HLM. A, Representative FISH (upper panels) and IHC (lower panels) analysis for HMGA2 overexpression. Myometrial (Myo) cells showed colocalization of hybridization signals producing a yellow color, or direct juxtaposition of red and green signals, indicating intact *HMGA2* and immunonegativity for HMGA2. HLM cases negative for *HMGA2* rearrangement showed tumor cells with similar patterns to the control. HLM cases positive for *HMGA2* rearrangement showed tumor cells with separate hybridization signals producing single spectrum-green and spectrum-orange colors in a typical pattern (dashed circles) with lack of signal location overlap. Immunoreactivity for HMGA2 overexpression in HLM cases is also illustrated below. B, Distribution of *MED12* mutations in exon 2 is illustrated. Upper panel represented no mutation in 21 HLMs, and lower panel showed 15 point mutations in different locations of ULM. Magnification indicated in the right lower corner by the black bar (500 μm).

or mucin was seen. Tumors lacked gross infiltrative features, but extrauterine cases were associated with surrounding adhesions.

Histologic and cytologic features of HLM cases were unsurprisingly similar to those reported by Clement et al [3] (Figs. 1 and 2). The monomorphic smooth muscle tumor cells had small rounded and oval nuclei with varied growth patterns and hypercellular and hypocellular arrangement in the background of edema or loose hyaline extracellular matrix (Figs. 1 and 2). In comparison to ULM, HLM displayed a background of increased edema in poorly delineated areas most readily appreciated in low-power fields. HLM cases with high edematous change (scores 2+ and 3+) and low edematous change (scores 0 and 1+) each numbered 12 (50%) of 24 compared with ULM cases, with few containing high change (3/21 [14%]) and most containing low change (18/21 [18%]; $P < .001$; Table). Intermixed within edematous areas were tumor cells arranged predominantly in cords with/or without perinodular growth around vessels. HLM tumors showed increased vascularity compared with ULM. HLM cases showed an average of 17 thick-walled vessels/10× mpf (range, 7-40 vessels) compared with 9/10× mpf (range, 0-21 vessels) seen in ULM ($P < .001$). Collections of tumor cells largely did not display ULM fascicular architecture.

In addition, we found that HLM tumor cells contained mostly round-oval nuclei with pinpoint nucleoli and a relatively low mitotic count (up to 2/10 hpf). Typical smooth muscle nuclear features were not readily appreciated. No nuclear atypia or bizarre nuclear features were seen. Only 2 cases showed areas of ischemic necrosis.

3.3. Analysis of HMGA2 overexpression, *MED12* mutation, and loss of *FH*

Alterations of *MED12*, *HMGA2*, and *FH* account for more than 80% of ULMs [7]. To investigate these 3 driver gene alterations in HLM, we conducted gene mutation analyses in all cases. Biallelic loss of FH expression was evaluated by IHC

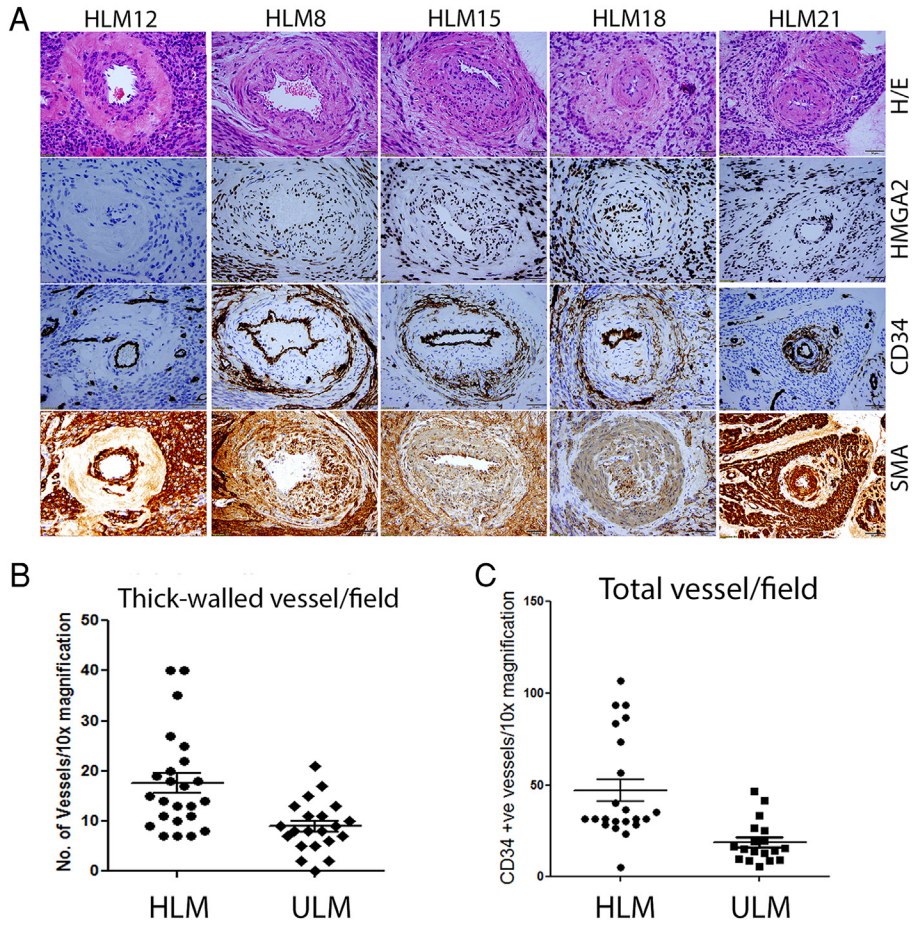

Fig. 4 IHC analysis of characteristic thick-walled vessels and vessel density in HLM and ULM. A, Vessels from 4 HLM cases are strongly immunoreactive for HMGA2, including intramural tumor cells of vasculature and perivascular tumor cells (second to fifth columns). The same cases show that perivascular pericytes are positive for CD34 immunostain in tumor vessels, which are positive for HMGA2 overexpression. In comparison, one HLM case negative for HMGA2 immunostain displays no CD34-positive pericytes around thick-walled vessels (first column). B, Dot plot illustrating the vessel density in HLM and ULM counted under microscope in ×10 magnification. C, Dot plot illustrating the vessel density in HLM and ULM detected by immunostain for CD34. Magnification indicated in the right lower corner by the black bar (50 μm).

only. We found that 100% of both HLMs (24/24) and ULMs (21/21) were positive for FH expression (Table).

HMGA2 overexpression was first evaluated via IHC and defined by strong and diffuse immunoreactivity in tumor cell nuclei (Fig. 3A). Remarkably, 18 (76%) of 24 HLM tumors showed high levels of HMGA2, with 6 (24%) of 24 showing absent to low levels of expression (Table). To confirm the IHC results obtained on TMA sections, whole-mounted tumor sections from all cases were performed and similar findings were observed.

To further investigate whether HMGA2 overexpression in HLM was due to *HMGA2* rearrangement (translocation), FISH testing for *HMGA2* rearrangement was performed on TMA tissue sections of all 24 HLM cases, and of these, 19 cases showed definite results. Six of (32%) 19 cases were positive for *HMGA2* gene rearrangement with an average of 31% positivity cells (range, 18.5%-41%), and 43% HMGA2-positive tumors had gene rearrangement (6/14; Table and Fig. 3B). All Müllerian controls were negative for *HMGA2* rearrangement.

Assessment of MED12 IHC showed varied immunoreactivity in all HLM and ULM cases. Semiquantitiave analysis revealed that strong immunoreactivity for MED12 was observed in 11 (46%) of 24 HLM cases, with 13 (54%) of 24 showing low-moderate immunoreactivity. In comparison, only 4 (19%) of 21 ULM cases showed strong MED12, whereas most (17/21 [81%]) showed low-moderate immunoreactivity (Table). To further evaluate *MED12*, *MED12* mutations were examined by Sanger sequencing in 21 HLMs, and all showed no exon 2 mutations in *MED12* (0/21 [0%]). In comparison, ULM controls showed exon 2 mutations in *MED12* in 15 (71%) of 21 ($P < .001$; Table and Fig. 3B).

3.4. Additional IHC analysis of the select ULM-associated markers

To further evaluate ULM-associated biomarkers in HLM, additional IHC analysis was performed including ER, pAKT, and Ki-67. Some degree of ER expression was observed in all HLM and ULM cases; however, on average, a greater immunopercentage for ER was seen in HLM (80%) compared with ULM (60%; $P = .004$; Table). Higher levels of pAKT were seen in HLM tumors (3.0) compared with ULM tumors (1.0; $P < .001$; Table). Similarly, Ki-67 staining showed a slightly higher proliferation index in HLM cases (average 4%) compared with that in ULM cases (average 2%; $P = .021$).

HLM tumor-vessel density was further evaluated using CD34 and SMA immunostains. With IHC, vascular density was evaluated across three 20× mpfs and counted as total number of both thick-walled and thin-walled vessels per mpf. HLM cases showed increased vascular density, an average of 47 vessels/20× mpf (range, 5-106 vessels), compared with ULM cases, which showed 22 vessels/20× mpf (range, 6-80 vessels; $P = .0003$; Table). Cells comprising the walls of thick-walled vasculature in HMGA2-positive HLM cases were positive for both HMGA2 and SMA (Fig. 4), suggesting the abnormal vessel formation from tumor cells. A distinct perivascular rim/layer of CD34-positive cells was also observed in HMGA2-positive HLM cases, but not in HMGA2-negative tumors (Fig. 4). Moreover, cells comprising walls of thick-walled vasculature in HMGA2-negative HLM cases were negative for HMGA2 and positive for SMA, and no rim/layer of CD34-positive cells was seen (Fig. 4).

3.5. Therapy and follow-up

All of the patients in our study underwent surgery as definitive management for their disease. Eleven (46%) of 24 patients underwent myomectomy only, and the remaining 13 (54%) of 24 underwent hysterectomy. Immediate and short-term postoperative data were available for 20 (83%) of 24 patients. Most patients experienced an uncomplicated clinical course. Those with postoperative complications had events including 2 wound separations without dehiscence or infection, 1 vaginal cuff cellulitis, 1 urinary tract infection, and 1 ileus versus bowel obstruction. The patient who presented during pregnancy had a normal remaining pregnancy carried to term delivery. In addition, long-term follow-up (>1 year since procedure/diagnosis) data were available for 7 (29%) of 24 patients, and all showed benign clinical course with no evidence of disease recurrence. Similar benign disease status is seen in 9 (37%) of 24 patients who underwent their respective procedures and were diagnosed as having HLM in the year 2017.

4. Discussion

Current studies have shown that 60% to 70% of leiomyomata harbor *MED12* mutations [7,8], whereas 10% to 15% gain *HMGA2* overexpression because of t(12;14) translocation [5], and less than 1% show biallelic loss of FH. These genetic alterations are mutually exclusive, indicating different driving forces for tumorigenesis and biologic behavior [5,6]. Most notably, molecular analysis shows that tumors with *HMGA2* overexpression have significantly larger size than those harboring *MED12* mutations [5]. Recognizing leiomyomata with *HMGA2* overexpression can thus be an important factor in predicting tumor growth and behavior, especially in myomectomy specimens. Upon review of the literature, we found HLM to cause a distressing symptomatic burden on patients, similar to clinically impactful leiomyomata with *HMGA2* overexpression previously studied. Clinical presentations and workup are additionally concerning given the often large masses seen, overlap with features of female reproductive tract malignancies, and requirement of interventional surgical therapy. Because of HLM's clinical significance, we initiated this study.

Our patient population overall was found to be similar to the patients seen in reported HLM cases from the literature. The patients in our series clinically presented as women of

reproductive age (average age, 43.79 ± 12.7 years), similar to the reported cases from the literature with a median age 42 years (range, 26-50 years) [4,9-19]. Presenting symptoms of our patients and reported cases resembled those of other female reproductive organ masses [9-18]. Interestingly, one patient's HLM from this study and 3 reported cases manifested during pregnancy either as acute or chronic complications [10-12]. Another unexpected presentation observed in reported cases (7 in total) was pseudo-Meigs syndrome: shortness of breath and pleural effusion with a concurrent pelvic or abdominal mass, elevated serum CA-125, and, in some patients, ascites [13-15].

Another consistency between the literature and our study was the overlap of HLM with features concerning for gynecologic malignancies. Physical examination data depicted most patients having large, painless pelvic or abdominal masses that were occasionally mobile and often obscuring normal reproductive organ anatomy [9,10,13-15,19]. Imaging studies ranged from well-demarcated uterine tumors to multinodular and complex exophytic masses blurring adnexae and on occasion displacing nearby organs [9,10,17-19], as well as showing degenerative or cystic changes similar to malignancy like leiomyosarcoma [9-12,14]. Given these findings, women could easily be referred to the gynecologic oncology for treatment, 5 patients in our study. Patient follow-up data from our population and reported cases, including those with pseudo-Meigs syndrome and pregnancy complications, were benign with no overt disease recurrence after surgery [9,12-16,19].

We found HLM to contain characteristic gross and histologic features. Tumors from our series were on average larger in size than ULM (14.4 ± 8.2 cm versus 6.7 ± 0.8 cm, respectively), with some HLM in our patients reaching 34 cm. Similarly, reported cases in the literature show large tumors with a median size of 17 cm (range, 4.2-30 cm) [4,9-19]. Grossly, HLM showed well-demarcated, vaguely lobulated tumors containing intact overlying serosa in relevant cases and white-gray to gray-tan cut surfaces with watery edema [4,9-12,15-19]. Additional previously reported abnormalities include contain gross cysts with gelatinous to watery fluid [9,12,15] and the overt presence of vessels [5-6,14]. These findings should be readily apparent as they are different from the typical firm, whorled, white-pink gross features of ULM in comparison.

The architectural features of HLM we identified in our study were similar to those reported by Clement et al [3]. We appreciated HLM tumor features for the most part to replace those typically observed in ULM. Moreover, we identified an additional cytologic feature in all cases that tumor cell nuclei were round-oval with pinpoint nucleoli more reminiscent of myofibroblasts (Fig. 2). The classic smooth muscle, cigar-shaped nuclei of tumor cells were less appreciated. More in line with the description by Clement et al, we observed low mitoses or no bizarre nuclear features in HLM. A single previously described case revealed focal severe nuclear atypia and multinucleated giant cells [19]. Overall, the cytologic features of HLM should convey its benign disease nature despite the typically concerning clinical features on presentation.

We found vessel density to be significantly higher in HLM than in ULM, also in line with the observations of Clement et al. HLM consists of 17 thick-walled vessels/10× mpf compared with 9/10× mpf in ULM. IHC highlighted thin vasculature also and revealed HLM to contain on average 47 vessels/three 20× mpf against 22 vessels/three 20× mpf in ULM. The vessels occurred throughout tumor sections. However, tumor cells were most prominently concentrated around vessels. HLM also displayed more edema than did ULM, and edematous areas within tumor sections were both less dense in vasculature and paucicellular. Vessels were not overtly compressed by edematous stroma, but tumor cells were pushed into cords. It is reasonable to infer that the HLM's increased vasculature plays a significant role in the augmented volume of edema seen in comparison to ULM. We propose that the tumor thick-walled vessels in HLM are defective by poorly organized intima with tumor cells (Fig. 4), and thus fluid leaking out of them regularly produces abnormally expanded stroma. This concept would readily explain the large volume of HLM versus ULM, which is usually lacking in significant vasculature. In relation to the prominent vessels seen in HLM, we discovered 2 new findings in this entity that may help explain tumorigenesis through HMGA2 overexpression. The exact mechanism of how HMGA2 promoting large and vascular HLM deserves further investigation.

By IHC testing in our patient population, 76% of HLMs showed HMGA2 overexpression. Tumor cells growing in cords, as perivascular nodules, and comprising the walls of thick-walled vasculature were all appreciated to be equally positive (Fig. 4). Moreover, tumor cells within vessel walls were also SMA+ and CD34−. Immunohistochemical stains further not only highlighted endothelial cells, which were SMA− and CD34+, but also highlighted a rim/perivascular layer of CD34+ cells (Fig. 4). This cellular rim was identified in HMGA2-positive HLM cases and lacking in all HMGA2-negative cases. We believe these cells to be tumor vessel–supporting pericytes/tumor stem cells that play a role in tumorigenesis by maintaining vascularity or tumor progenitor cells to HLM. This would ultimately allow tumors to grow to large sizes. Also, if these defective vessels are maintained as we suspect, that would allow for more edema leakage into stroma, adding even more to tumor size.

We evaluated *HMGA2* status in HLM using FISH break-apart probes at 12q14.3. This gene codes for a high-mobility group protein involved in enhancing DNA architecture for replication by regulatory effects on transcription factors [20]. Involved in mesenchymal development and not normally expressed in mature tissue, *HMGA2* has been shown to be rearranged in multiple mesenchymal tumors, including uterine leiomyomas [5,6,20]. *HMGA2* acts as a driver gene in tumors that harbor chromosomal rearrangements, including translocations and other complex abnormalities, at 12q14-15 [7,21]. The break-part probes for *HMGA2* we used showed gene rearrangement in 32% of all HLMs and 43% of HMGA2-positive HLMs. This finding suggests that other mechanisms leading to HMGA2 overexpression in HLM may exist. We also noted that HLM had high pAKT levels and increased KI-67 index

in comparison to ULM, indicating a strong contribution of AKT pathway signaling in HLM. Interestingly, these findings in HLM were consistent with the observation from ULM with HMGA2 overexpression. In a separate study, we examined the difference of the selected gene pathways in ULM with 3 driver gene mutations/alteration, including *MED12*, *HMGA2*, and *FH.* We found that leiomyoma with HMGA2 overexpression had significantly higher AKT signaling than did those leiomyomas with *MED12* or *FH* alteration [22].

Our findings overall suggest that HMGA2 may assist in the diagnostic workup of HLM. This concept is especially true in biopsy specimens or myomectomies. Considering that the characteristic features of HLM occur in zonal distributions depending on the extent of edematous change, HLM can indeed be a diagnostic challenge. The differential diagnosis for HLM most readily includes entities: angiomyxoma, angioleiomyoma, and myxoid leiomyoma. Based on observations from prior studies and our current series, the differing characteristic histologic features of HLM and ancillary studies, such as IHC, should facilitate diagnostic accuracy.

To our knowledge, our study of 24 cases is the largest series analysis of HLM to date. We found data from our patient cohort that are consistent with knowledge regarding HLM previously reported in the literature, as well as some novel observations that potentially help clarify tumor biogenesis and aid in diagnostic assistance and patient management. In summary, HLM is a variant of leiomyoma with characteristic morphologic features helpful for proper diagnosis. Our data suggest that HLM is likely driven by HMGA2 overexpression, possibly explaining this entity's augmented disease burden and pathologic findings in comparison to ULM. An essential aspect of HLM seems to be increased thick-walled vasculature, not only composed of HMGA2+ tumor cells but also supported by CD34+ pericytes. Further studies are warranted to better understand HLM biology and its clinical translation.

Supplementary data

Supplementary data to this article can be found online at https://doi.org/10.1016/j.humpath.2018.09.012.

Acknowledgments

We acknowledge technical support for this study from Northwestern University's Pathology Core Facility and NUSeq core.

References

[1] Styer AK, Rueda BR. The epidemiology and genetics of uterine leiomyoma. Best Pract Res Clin Obstet Gynaecol 2016;34:3-12.

[2] Kurman RJ, Carcangiu ML, Herrington CS, Young RH. WHO Classification of Tumours of Female Reproductive Organs. 4th ed. Lyon: IARC; 2014. p. 137.

[3] Clement PB, Young RH, Scully RE. Diffuse, perinodular, and other patterns of hydropic degeneration within and adjacent to uterine leiomyomas. Problems in differential diagnosis. Am J Surg Pathol 1992;16:26-32.

[4] Van den Berghe I, Dal Cin P, Sciot R, et al. Translocation (4;8) as a primary chromosome change in a hydropic leiomyoma. Histopathology 1999;34:378.

[5] Bertsch E, Qiang W, Zhang Q, et al. MED12 and HMGA2 mutations: two independent genetic events in uterine leiomyoma and leiomyosarcoma. Mod Pathol 2014;27:1144-53.

[6] Makinen N, Kampjarvi K, Frizzell N, Butzow R, Vahteristo P. Characterization of MED12, HMGA2, and FH alterations reveals molecular variability in uterine smooth muscle tumors. Mol Cancer 2017;16:101.

[7] Mehine M, Kaasinen E, Makinen N, et al. Characterization of uterine leiomyomas by whole-genome sequencing. N Engl J Med 2013;369:43-53.

[8] Makinen N, Mehine M, Tolvanen J, et al. MED12, the mediator complex subunit 12 gene, is mutated at high frequency in uterine leiomyomas. Science 2011;334:252-5.

[9] Horta M, Cunha TM, Oliveira R, Magro P. Hydropic leiomyoma of the uterus presenting as a giant abdominal mass. BMJ Case Rep 2015;2015:5.

[10] Heffernan E, Kobel M, Spielmann A. Case report: hydropic leiomyoma of the uterus presenting in pregnancy: imaging features. Br J Radiol 2009;82:e164-7.

[11] Awad EE, El-agwany AS, Elhabashy AM, El-zarka A, Moneim ASA. A giant uterine myometrium cyst mimicking an ovarian cyst in pregnancy: an uncommon presentation of hydropic degeneration of uterine fibroid. Egypt J Radiol Nucl Med 2015;46:529-34.

[12] Moore L, Wilson S, Rosen B. Giant hydropic uterine leiomyoma in pregnancy: unusual sonographic and Doppler appearance. J Ultrasound Med 1994;13:416-8.

[13] Dunn Jr JS, Anderson CD, Method MW, Brost BC. Hydropic degenerating leiomyoma presenting as pseudo-Meigs syndrome with elevated CA 125. Obstet Gynecol 1998;92:648-9.

[14] Amant F, Gabriel C, Timmerman D, Vergote I. Pseudo-Meigs' syndrome caused by a hydropic degenerating uterine leiomyoma with elevated CA 125. Gynecol Oncol 2001;83:153-7.

[15] Oguma T, Yamasaki N, Nakanishi K, Kinoshita D, Mitsuhashi T, Nakagawa S. Pseudo-Meigs' syndrome associated with hydropic degenerating uterine leiomyoma: a case report. J Obstet Gynaecol Res 2014;40:1137-40.

[16] Ceyhan K, Simsir C, Dolen I, Calyskan E, Umudum H. Multinodular hydropic leiomyoma of the uterus with perinodular hydropic degeneration and extrauterine extension. Pathol Int 2002;52:540-3.

[17] Coad JE, Sulaiman RA, Das K, Staley N. Perinodular hydropic degeneration of a uterine leiomyoma: a diagnostic challenge. Hum Pathol 1997;28:249-51.

[18] Roth LM, Reed RJ. Dissecting leiomyomas of the uterus other than cotyledonoid dissecting leiomyomas: a report of eight cases. Am J Surg Pathol 1999;23:1032-9.

[19] Jashnani KD, Kini S, Dhamija G. Perinodular hydropic degeneration in leiomyoma: an alarming histology. Indian J Pathol Microbiol 2010;53:173-5.

[20] Fusco A, Fedele M. Roles of HMGA proteins in cancer. Nat Rev Cancer 2007;7:899-910.

[21] Ligon AH, Morton CC. Genetics of uterine leiomyomata. Genes Chromosomes Cancer 2000;28:235-45.

[22] Xie J, Ubango J, Ban Y, Chakravarti D, Kim JJ, Wei JJ. Comparative analysis of AKT and the related biomarkers in uterine leiomyomas with MED12, HMGA2, and FH mutations. Genes Chromosomes Cancer 2018;57:485-94.